MOLECULAR AND CELLULAR BIOLOGY, Sept. 1996, p. 4869–4878 Vol. 16, No. 9
0270-7306/96/$04.00+0

The Ras GTPase-Activating-Protein-Related Human Protein IQGAP2 Harbors a Potential Actin Binding Domain and Interacts with Calmodulin and Rho Family GTPases

SUZANNE BRILL,[1] SHIHONG LI,[1] CHARLES W. LYMAN,[1] DEANNA M. CHURCH,[2] JOHN J. WASMUTH,[2] LAWRENCE WEISSBACH,[3] ANDRÉ BERNARDS,[1]* AND ALLARD J. SNIJDERS[1]

Massachusetts General Hospital Cancer Center, Harvard Medical School,[1] and Orthopedic Research Laboratories,[3] Massachusetts General Hospital, Charlestown, Massachusetts 02129 and Department of Biological Chemistry, College of Medicine, University of California—Irvine, Irvine, California 92717[2]

Received 9 May 1996/Returned for modification 5 June 1996/Accepted 18 June 1996

We previously described IQGAP1 as a human protein related to a putative Ras GTPase-activating protein (RasGAP) from the fission yeast *Schizosaccharomyces pombe*. Here we report the identification of a liver-specific human protein that is 62% identical to IQGAP1. Like IQGAP1, the novel IQGAP2 protein harbors an N-terminal calponin homology motif which functions as an F-actin binding domain in members of the spectrin, filamin, and fimbrin families. Both IQGAPs also harbor several copies of a novel 50- to 55-amino-acid repeat, a single WW domain, and four IQ motifs and have 25% sequence identity with almost the entire *S. pombe* sar1 RasGAP homolog. As predicted by the presence of IQ motifs, IQGAP2 binds calmodulin. However, neither full-length nor truncated IQGAP2 stimulated the GTPase activity of Ras or its close relatives. Instead, IQGAP2 binds Cdc42 and Rac1 but not RhoA. This interaction involves the C-terminal half of IQGAP2 and appears to be independent of the nucleotide binding status of the GTPases. Although IQGAP2 shows no GAP activity towards Cdc42 and Rac1, the protein did inhibit both the intrinsic and RhoGAP-stimulated GTP hydrolysis rates of Cdc42 and Rac1, suggesting an alternative mechanism via which IQGAPs might modulate signaling by these GTPases. Since IQGAPs harbor a potential actin binding domain, they could play roles in the Cdc42 and Rac1 controlled generation of specific actin structures.

Members of the Ras GTPase superfamily function as binary switches in diverse biological processes (8). Critical to this switching role is the ability of these GTPases to cycle between inactive GDP- and active GTP-bound states. Important mediators of this cycling include exchange factors, which activate Ras-related GTPases by promoting exchange between the bound nucleotide and a cytoplasmic GTP pool, and GTPase-activating proteins (GAPs), which accelerate their intrinsic GTPase activity, leading to their inactivation (6).

Although members of the Ras superfamily show extensive similarity (9), exchange factors and GAPs for different subgroups within the Ras superfamily have been mostly unrelated in sequence (6). Our previous identification of human IQGAP1 as a protein related to a RasGAP homolog from *Schizosaccharomyces pombe* therefore predicted a role as a novel Ras regulator (48). Since GAPs are important regulators and perhaps also effectors of GTPase-controlled signaling pathways (7, 32), and because the precedent of the neurofibromatosis 1 protein suggested that other RasGAPs might be tumor suppressors, we have been interested in further defining the role of IQGAP1 in GTPase-mediated processes. During this study we identified cDNAs predicting a highly related human IQGAP2 protein. Here we present our characterization of this novel liver-specific protein, which is 62% identical to IQGAP1. Confirming what we previously found for IQGAP1, IQGAP2 shows no in vitro GAP activity towards Ras or its immediate relatives. Instead IQGAP2 interacts with G25K/Cdc42Hs (hereafter called Cdc42) and Rac1 but not with RhoA. This finding and the presence of a potential actin binding domain suggest that IQGAPs could play roles in the as yet poorly understood mechanisms via which Rho-family GTPases control the generation of specific polymerized actin structures.

* Corresponding author. Mailing address: MGH Cancer Center, Building 149, 13th St., Charlestown, MA 02129. Phone: (617) 726-5620. Fax: (617) 724-9648. Electronic mail address: abernards@helix.mgh.harvard.edu.

MATERIALS AND METHODS

DNA and RNA analysis. Two partial IQGAP2 cDNAs were identified during the screening of a mouse brain library with a human IQGAP1 probe under conditions of relaxed stringency. Subsequent screens of oligo(dT)- and randomly primed human liver cDNA libraries purchased from Stratagene and Clontech yielded 67 and more than 250 positive clones, respectively. Approximately 70% of the 5,767-bp IQGAP2 cDNA sequence was determined on both strands by chain termination sequencing of 30 unique partial cDNA clones with T3 and T7 primers. Gaps in the double-stranded sequence were filled by sequencing subclones and by using custom oligonucleotides as sequencing primers. The chromosomal location of IQGAP2 was determined by DNA blot analysis, using *Eco*RI-digested DNAs from 43 rodent-human somatic cell hybrid lines (references 21 and 38; also National Institute of General Medical Sciences mapping panel 2, Coriell Institute, Camden, N.J.). Confirmation of the mapping to chromosome 5 was obtained by analyzing additional hybrids containing defined chromosome 5 translocation and deletion mutants (34). Blots were hybridized with a human IQGAP2 cDNA fragment (bp 1406 to 3404) at 42°C in hybridization buffer containing 50% formamide and washed in 0.25× SSC (1× SSC is 0.15 M NaCl plus 0.015 M sodium citrate) at 65°C. Probes were radioactively labeled by the random-priming protocol (18). IQGAP2 mRNA expression was analyzed by hybridizing murine multiple tissue RNA blots (Clontech) under high-stringency conditions with a cDNA fragment representing the sar1-homologous part of mouse IQGAP2. Total RNA was made by lysing cells in 4 M guanidinium thiocyanate, and this was followed by centrifugation through a 6.2 M CsCl cushion. RNAs were size separated on 1% formaldehyde agarose gels, transferred to nylon filters, and hybridized with randomly primed probes by standard procedures (42).

Generation of IQGAP2 constructs. Four partial IQGAP2 cDNAs were ligated to generate a full-length construct in the pBSK(−) vector (Stratagene). The integrity of this and all subsequent constructs was verified by sequence analysis. A hemagglutinin (HA) tag was added to the extreme end of the reading frame by PCR amplification with an IQGAP2-HA hybrid primer (GAT CGG TAC

CTC AGC TAG CGT AAT CTG GAA CAT CGT ATG GGT ACT TTC CAT AGA ACT TCT TGT TCA). The underlined sequence is a unique *Kpn*I site which was included for cloning purposes. To generate an IQGAP2-HA mammalian expression vector, the tagged cDNA was digested with *Kpn*I and *Bam*HI (which cuts in the 5′ untranslated segment of IQGAP2 cDNA) and ligated into a *Bam*HI- and *Kpn*I-digested simian virus 40 promoter-driven pJ3Ω expression vector (33).

Vectors to express truncated IQGAP2 proteins were generated as follows. The IQGAP2-N vector was made by deleting the segment encoding amino acids 789 to 1509 from the full-length HA-tagged expression vector. This was done by digesting a C-terminal IQGAP2 cDNA with *Bst*1107I and *Eco*RV and then performing recircularization. This deleted C-terminal construct was then used to remake the full-length expression vector. Similarly, the IQGAP2-C1 vector was made by transferring a 3′ *Sac*I-*Kpn*I fragment of the HA-tagged cDNA to the pJ3Ω vector. The first AUG codon downstream of the *Sac*I site occurs at codon 711 within the second IQ motif. Finally, the IQGAP2-C2 construct was designed to more precisely represent the sar1-homologous segment of the protein. Since no convenient cloning sites or potential start codons occurred near the start of this segment, we performed PCR amplification with a synthetic primer (AC GCG TCG ACG ACG CGC AGG ATG GTG AAC CTG ATG GAC ATC AAG ATT GGA CTG) to add a *Sal*I site and an in-frame start codon (both underlined; the start codon and flanking sequence added are identical to the region around the first AUG codon in the IQGAP2 reading frame). The *Sal*I-*Kpn*I fragment representing the sar1-homologous part of IQGAP2 (amino acids 826 to 1657, followed by the HA tag) was initially subcloned into pBSK and subsequently transferred to the pJ3Ω vector, after digestion with *Sma*I, which cuts in the pBSK polylinker, and *Kpn*I.

To produce full-length IQGAP2 or its sar1-homologous C-terminal segment in the baculovirus system, two constructs were made in the pAcSG His NT-A and pAcSG His NT-B transfer vectors (Pharmingen). These vectors add six consecutive histidine residues to the N termini of the inserted proteins, which allows their purification by nickel-resin affinity chromatography (24). Both constructs also included a C-terminal HA tag. Generation of recombinant baculovirus and amplification of the recombinant virus were performed as recommended by the manufacturer.

Purification of baculovirus proteins. Hi-5 or Sf9 insect cells were plated at a density of 2×10^7 cells per 15-cm-diameter culture dish and infected with baculovirus stocks at a multiplicity of infection of 10. After 40 h at 27°C, cells were harvested by spritzing in medium and were collected by centrifugation. The cell pellet was resuspended in buffer containing 50 mM sodium phosphate (pH 7.8), 50 mM sodium chloride, 1 mM phenylmethylsulfonyl fluoride, 1 mM β-mercaptoethanol, and 10 μg each of aprotinin, chymostatin, and antipain per ml. Cells were lysed by freeze-thawing and sonication, and debris was removed by centrifugation. Cleared lysate was incubated for 1 h at 4°C with nickel-nitrilotriacetic acid resin (Qiagen) in the presence of 150 mM sodium chloride, 0.1% (vol/vol) Nonidet P-40, and 30 mM imidazole. Beads were washed extensively, and bound proteins were eluted with a stepwise gradient of imidazole (50 to 200 mM) in buffer containing 50 mM sodium phosphate, 300 mM sodium chloride, 10% (vol/vol) glycerol, 0.1% (vol/vol) Nonidet P-40, 1 mM phenylmethylsulfonyl fluoride, and 1 mM β-mercaptoethanol. Fractions containing IQGAP2 (as determined by Coomassie staining of sodium dodecyl sulfate [SDS] gels or by blotting) were pooled and dialyzed against buffer containing 50 mM Tris HCl (pH 7.4), 50 mM sodium chloride, 5 mM magnesium chloride, and 1 mM β-mercaptoethanol. The protein was concentrated with a Centricon-30 filter (Amicon) and stored at −135°C.

GST fusion protein binding assays. Glutathione *S*-transferase (GST)–GTPase fusion proteins were produced in *Escherichia coli* carrying pGEX vectors as previously described (41). For bead-binding assays, fusion proteins were bound to glutathione agarose for 1 h at 4°C. Beads were washed extensively in buffer containing 50 mM Tris HCl (pH 7.4), 50 mM sodium chloride, 5 mM magnesium chloride, 1 mM dithiothreitol, and 1 mM phenylmethylsulfonyl fluoride and stored at 4°C as a 50% slurry for up to 2 weeks.

To GDP or GTP load fusion proteins, 20-μl aliquots of the suspensions described above were briefly centrifuged to remove excess buffer. To the packed beads on ice were then added 39 μl of binding buffer (25 mM NaCl, 20 mM Tris HCl [pH 7.5], 0.1 mM dithiothreitol), 5 μl of 50 mM EDTA, and 1 μl of 50 mM GDP or guanylyl imidodiphosphate (GMP-PNP) (Boehringer). The mixture was incubated at 30°C for 10 min, and the reaction was stopped by addition of 12.5 μl of 0.1 M $MgCl_2$. The beads were subsequently incubated with 0.2 ml of infected insect cell lysate for 2 h at 4°C in GAP lysis buffer (50 mM HEPES [*N*-2-hydroxyethylpiperazine-*N*′-2-ethanesulfonic acid] [pH 7.4], 150 mM sodium chloride, 1.5 mM magnesium chloride, 5 mM EGTA [ethylene glycol-bis(β-aminoethyl ether)-*N*,*N*,*N*′,*N*′-tetraacetic acid], 10% glycerol, 1% Triton X-100, 1 mM phenylmethylsulfonyl fluoride, and 10 μg each of aprotinin, chymostatin, and antipain per ml), collected by centrifugation, and washed three times with 1 ml of IP wash buffer (20 mM HEPES [pH 7.4], 150 mM NaCl, 10% glycerol, 0.1% Triton X-100). Bound proteins were analyzed by SDS-polyacrylamide gel electrophoresis (PAGE) and immunoblotting after the beads were boiled in SDS sample buffer.

GAP assays. For GAP assays, active GTPase concentrations of thrombin-cleaved proteins were determined by ^{3}H-GTP binding in a filter-binding assay (22). GAP assays were performed by mixing on ice 14.6 μl of binding buffer (25 mM NaCl, 20 mM Tris HCl [pH 7.4], 0.1 mM dithiothreitol), 2 μl of 50 mM EDTA, 1 μl of [γ-^{32}P]GTP (6,000 Ci/mmol; New England Nuclear), and 4 μl of thrombin-cleaved GST-GTPases (0.008 mg/ml). After a 10-min incubation at 30°C, the reactions were stopped by adding $MgCl_2$ to 20 mM. Proteins were then tested for GAP activity by mixing infected insect cell lysates or affinity-purified proteins on ice with 3 μl of GTP-loaded GTPases in a total volume of 30 μl containing 1 mg of bovine serum albumin per ml and 1 mM nonradioactive GTP, giving a final GTPase concentration of approximately 6 nM. GAP activity was measured by withdrawing aliquots before and after a brief incubation at 23°C, or at 30°C in the case of Ras. Aliquots were diluted in 1 ml of wash buffer (50 mM sodium chloride, 50 mM Tris-HCl [pH 7.4], 5 mM magnesium chloride) and filtered through nitrocellulose membranes (BA 85; Schleicher and Schuell). Filters were washed with 10 ml of ice-cold wash buffer and air dried, and filter-bound radioactivity was quantitated by liquid scintillation counting.

Expression experiments. Subconfluent Cos cells were transfected by the DEAE-dextran method and processed for immunoprecipitation or immunoblotting as described previously (43). Briefly, cells were lysed in GAP lysis buffer, scraped from the dish, and centrifuged at $10,000 \times g$ for 20 min to remove debris. The resulting lysate was used immediately for GST fusion protein binding or immunoprecipitation procedures. For binding assays, lysate was precleared by incubation for 1 h at 4°C with GST bound to glutathione agarose. The beads were removed by centrifugation, and the lysate was incubated with the appropriate GST-GTPase fusion protein bound to glutathione agarose for 2 h at 4°C. Beads were washed four times with IP wash buffer, prior to boiling in SDS sample buffer and analysis by SDS-PAGE. For immunoprecipitations, lysate was precleared for 1 h at 4°C with 20 μg of rabbit immunoglobulin G adsorbed onto protein A-Sepharose, and this was followed by incubation for 2 h at 4°C with 150 μl of culture supernatant of the mouse anti-HA monoclonal antibody 12CA5 or with 2 μl of two rabbit polyclonal anti-IQGAP2 peptide antisera (Research Genetics, Inc.). The latter sera were made by immunizing rabbits with a conjugated IQGAP2 N-terminal peptide (DDERLSAEEMDERRRQN [residues 19 to 35]). Precipitates were collected with protein A-Sepharose, washed six times in IP wash buffer, boiled in SDS sample buffer, and subjected to SDS-PAGE on 8% gels. For the GTPase binding experiments, gels were divided into upper and lower halves at the level of the 66-kDa marker and the upper portion was enhanced with Autofluor (National Diagnostics) and autoradiographed. Proteins in the lower part of the gel were electroblotted onto nylon membranes and analyzed by immunoblot analysis (ECL system; Amersham) using a mouse anti-GST monoclonal antibody (GST12; Santa Cruz Biotechnology). Calmodulin (CaM) was detected with an anti-bovine CaM monoclonal antibody (05-173; Upstate Biotechnology). Ca^{2+}-dependent electrophoretic mobility shifts were analyzed after adding 2 mM $CaCl_2$ or EGTA to proteins before boiling in SDS sample buffer (10).

Nucleotide sequence accession number. The GenBank accession number for the human IQGAP2 cDNA sequence is U51903.

RESULTS

Identification of IQGAP2. We previously reported the identification of a human protein that harbored potential CaM-binding IQ motifs upstream of a segment related to the catalytic domain of RasGAPs (48). During the characterization of cDNAs for this IQGAP1 protein, we also found two mouse clones that predicted a segment of a related protein. To facilitate the isolation of additional cDNAs, we used mouse tissue RNA blots to survey the expression pattern of the novel gene. By contrast to *IQGAP1*, which is especially highly expressed in lung, kidney, and placenta (48), the results in Fig. 1A suggest that *IQGAP2* is predominantly expressed in liver, although in additional blots an abundant, shorter mRNA was also detected in testis (not shown).

To further determine which liver cell types express *IQGAP2*, we isolated RNAs from several human liver cancer-derived cell lines. Blot analysis showed that two pediatric hepatoblastoma lines (HepG2 and Hu-H7) and one adult hepatocellular carcinoma (HCC) line (Hep3B) expressed high levels of *IQGAP2* mRNA, whereas two other HCC lines (Focus and SK-Hep1) showed no detectable expression (Fig. 1B). Because *IQGAP2* is expressed in at least some hepatocyte-derived hepatoblastoma and HCC cell lines, the liver-specific expression observed in Fig. 1A probably reflects expression in hepatocytes.

Since the RasGAP homology of IQGAP1 suggested a potential role as a tumor suppressor, we previously mapped the *IQGAP1* gene to human chromosome 15p-15q1.1 (48). In a similar analysis of 43 human-rodent somatic cell hybrids rep-

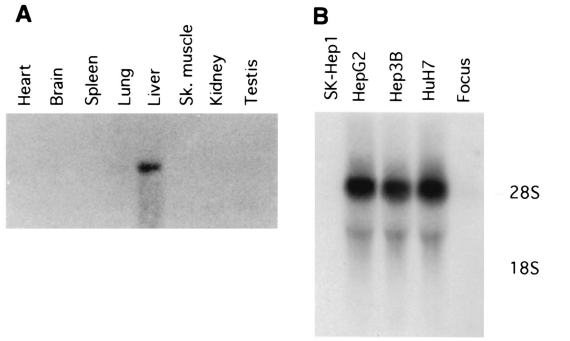

FIG. 1. IQGAP2 is expressed in mouse liver and human hepatocyte-derived cell lines. (A) Murine multiple tissue RNA blot (Clontech) containing poly(A) RNA from the indicated tissues after hybridization with a mouse IQGAP2 cDNA probe representing the sar1-homologous part of the protein. Sk. muscle, skeletal muscle. (B) Blot of size-fractionated total RNAs from the indicated human hepatoblastoma and HCC cell lines after hybridization with a human IQGAP2 cDNA probe. Control hybridizations with an actin probe confirmed that all lanes contained similar amounts of RNA (not shown).

resenting defined overlapping subsets of human chromosomes, all human *IQGAP2*-specific restriction fragments cosegregated with chromosome 5. To confirm this mapping and to further sublocalize the gene, we analyzed two hybrids containing chromosome 5 translocations and several hybrids harboring defined chromosome 5 deletions. This analysis confirmed the mapping of the *IQGAP2* gene to human chromosome 5 and allowed its sublocalization to the spinal muscular atrophy candidate region at 5q1.1-1.3 (results not shown). Although loss of heterozygosity of 5q markers is a frequent feature of some tumors, no allelic imbalance has been reported for polymorphic markers within the 5q1.1-1.3 interval in liver cancer. Moreover, analysis of the HCC cell lines that did not express *IQGAP2* mRNA revealed no obvious gene rearrangements (not shown).

To isolate clones representing the complete *IQGAP2* coding sequence, we screened two human liver cDNA libraries. Of the more than 300 clones identified in these screens, 40 were partially mapped and 30 were used to determine 5,767 bp of contiguous double-stranded *IQGAP2* cDNA sequence (GenBank accession number, U51903). Features of this sequence include a 222-bp GC-rich 5′ untranslated segment containing an in-frame stop codon, a 1,575-codon open reading frame, and 816 bp of 3′ untranslated sequence, ending in an oligo(A) stretch just downstream of a consensus AAUAAA poly(A) addition sequence. The predicted IQGAP2 protein (calculated molecular mass, 180,620 Da) is 62% identical and 77% similar to IQGAP1 over its entire length and harbors all domains previously identified in IQGAP1 (Fig. 2A). From the N to the C terminus, these include a so-called calponin homology (CH) domain, which is also present in Vav and in several actin-binding proteins, including members of the spectrin, filamin, and fimbrin families (Fig. 2B). The CH domain of IQGAP2 is followed by five copies of a novel 50- to 55-amino-acid repeat of unknown function, which we refer to as the IQGAP repeat domain (Fig. 2C), a single WW or WWP putative protein interaction domain (Fig. 2D), and four closely spaced IQ motifs, which have been implicated in CaM binding (Fig. 2E).

Beyond revealing the four types of domain within the N-terminal half of IQGAP2, database searches using the BLAST program (2) revealed additional similarities between IQGAP2 and two classes of proteins. Firstly, IQGAP1 and IQGAP2 each exhibit a low degree of similarity to several proteins that include α-helical coiled-coil segments, such as myosin heavy chains and intermediate filament proteins. These proteins contain typical heptad amino acid repeats, in which positions 1 and 4 are occupied by hydrophobic residues (28). Computer analysis of the IQGAP1 and -2 protein sequence indicates that several short segments have a high probability of forming coiled-coil structures (Fig. 2F). At least some of these segments are conserved between IQGAP1 and -2, and the related sar1 protein is predicted to also contain a similar short heptad repeat segment near its C terminus (not shown).

Secondly, IQGAPs also include an approximately 300-amino-acid segment related to the catalytic domains of RasGAPs. Among the 10 or so presently identified RasGAP-related proteins, IQGAPs are most closely related to a RasGAP homolog from *S. pombe*, called either sar1 (47) or gap1 (23). As in the case of the human neurofibromatosis type 1 and budding yeast IRA1 and IRA2 proteins, the sequence similarity between IQGAPs and sar1 is not confined to the putative catalytic segments of the proteins. Indeed, the protein sequence alignment in Fig. 3 demonstrates that IQGAP1 (top), IQGAP2 (middle), and sar1 (bottom) have 25% amino acid sequence identity from approximately 100 residues upstream of their putative catalytic segments (boxed in Fig. 3) all the way to their conserved C termini.

IQGAP2 binds CaM. IQ motifs are 30-amino-acid domains that serve as binding sites for CaM and related EF-hand proteins (13). To test whether IQGAP2 binds CaM, we transfected Cos-7 cells with HA-tagged full-length and truncated IQGAP2 expression vectors. Two days after transfection, cells were labeled and potential protein complexes were precipitated with the 12CA5 anti-HA monoclonal antibody. In these experiments, a prominent 17-kDa protein coprecipitated with full-length IQGAP2 but not with a truncated protein that lacked the IQ motifs (Fig. 4, left panel). The 17-kDa protein resembled CaM in size, and its interaction with IQGAP2 was not disrupted by washing the immunoprecipitates in 1% Triton and 0.6 M NaCl (14). The 17-kDa coprecipitating protein also showed a highly characteristic mobility shift when subjected to SDS-PAGE in the presence or absence of 2 mM Ca^{2+} (Fig. 4, lanes 2 and 3) and was unambiguously identified as CaM by probing blots of 12CA5 immunoprecipitates with the anti-CaM monoclonal antibody (Fig. 4, right panel). Evidence that IQGAP1 also interacts with CaM was obtained by performing a yeast two-hybrid screen with a bait that included the IQ motifs of this protein. The most frequent interactor identified in this screen was human CaM (data not shown).

IQGAP2 has no detectable in vitro RasGAP activity. To test whether IQGAP2 stimulates the GTPase activity of Ras, we produced both full-length and truncated proteins using the baculovirus expression system. Purification and detection of these proteins were facilitated by adding N-terminal six-histidine and C-terminal HA tags, respectively. In insect cells infected with full-length IQGAP2 recombinant baculovirus, a prominent 180-kDa anti-HA immunoreactive protein was readily detected (not shown). However, in multiple GAP assays either with unfractionated infected Sf9 or Hi-5 cell lysates or with a 10-fold molar excess of 70% pure full-length IQGAP2 purified by nickel affinity chromatography, no stimulation of the GTPase activity of thrombin-cleaved GST-H-Ras, GST-Rap1b, GST-TC21, or GST-RalA was observed under conditions under which a similar excess of p120GAP stimulated nearly 100% H-Ras-GTP hydrolysis (Fig. 5A). Identical results were obtained in the presence of exogenously added Ca^{2+}-CaM and in assays with a truncated baculovirus protein representing the sar1-homologous part of IQGAP2 (not shown). A large molar excess of affinity-purified full-length or truncated IQGAP2 also did not inhibit p120GAP-stimulated H-Ras-GTP hydrolysis under conditions under which a GST

A: Schematic structure:

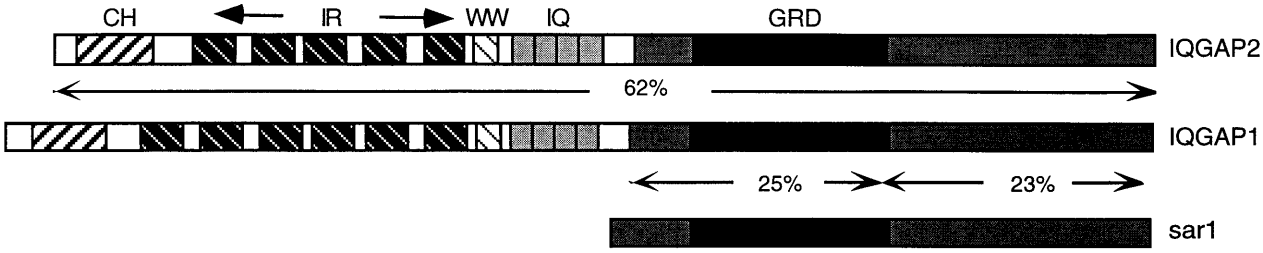

B: CH-domain:

```
IQGAP2     LEEAKRWMEV CLVEELPP.. ......TTEL EEGLRNGVYL AKLAKFFAPK MVSEKKIYDV
IQGAP1     LEEAKRWMEA CLGEDLPP.. ......TTEL EEGLRNGVYL AKLGNFFSPK VVSLKKIYDR
MP20       MDKEAQWIEA IEKFPAGQ.. .........SY EDVLKDGQVL CKLINVLSPN AVPKVNSSG.
Vav        WRQCTHWLIQ CRVLPPSHRV TWDGAQVCEF AQALRDGVLL CQLLNNLLPH AINLREVNL.
Calponin   EAELRSWIEG LTGLSI.... ......GPDF QKGLKDGVIL CTLMNKLQPG SVPKINRSM.
α-actinin  RKTFTAWCNS HLRKAGTQ.. ......IENI EEDFRDGLKL MLLLEVISGE RLAKPERGK.
Filamin    QNTFTRWCNE HLKCVSKR.. ......IANL QTDLSDGLRL IALLEVLSQK KMHRKHNQR.

IQGAP2     EQTRYKKSGL HFRHTDNTVQ WLRAMESI.G LPKIFYPETT DVYDRK..NI PRMIYCIHAL
IQGAP1     EQTRYKATGL HFRHTDNVIQ WLNAMDEI.G LPKIFYPETT DIYDRK..NM PRCIYCIHAL
MP20       .........G QFKFMENINN FQKALKEY.G VPDIDVFQTV DLYEKK..DI ANVTNTIFAL
Vav        .....RPQMS QFLCLKNIRT FLSTCCEKFG LKRSELFEAF DLFDVQ..DF GKVIYTLSAL
Calponin   .......... NWHKLENIGN FLRAIKHY.G VKHPDIFEAN DLFENT..NH TQVQSTLIAL
α-actinin  .........M RVHKISNVNK ALDFIASK.G VKLVSIGA.E EIVDGNVKMT LGMIWTLILR
Filamin    ........PTF RQMQLENVSV ALEFLDRE.S IKLVSIDS.K AIVDGNLKLI LGLIWTLILH
```

C: IR domains:

```
IQGAP2-1   AAVIAINEAV EKGIAEQTVV TLRNPNAVLT LVDDNLAPEY QKELWDAKKK
IQGAP2-2   AAVDHINAVI PEGDPENTLL ALKKPEAQLP AVYPFAAAMY QNELFNLQKQ
IQGAP2-3   SAVALLNQAL ESNDLVSVQN QLRSPAIGLN NLDKAYVARY ANTLLSVKLE
IQGAP2-4   AAVGYINEAI DEGNPLRTLE TLLLPTANIS DVDPAHAQHY QDVLYHAKSQ
IQGAP2-5   TLVVDVNQCL EGKKSSDILS VLKSSTSNAN DIIPECADKY YDALVKAKEL

IQGAP1-1   AAVIAINEAI DRRIPADTFA ALKNPNAMLV NLEEPLASTY QDILYQAKQD
IQGAP1-2   SALANIDLAL EQGDALALFR ALQSPALGLR GLQQQNSDWY LKQLLSDKQQ
IQGAP1-3   AAVALINAAI QKGVAEKTVL ELMNPEAQLP QVYPFAADLY QKELATLQRQ
IQGAP1-4   SSVALINRAL ESGDVNTVWK QLSSSVTGLT NIEEENCQRY LDELMKLKAQ
IQGAP1-5   LAIGLINEAL DEGDAQKTLQ ALQIPAAKLE GVLAEVAQHY QDTLIRAKRE
IQGAP1-6   LGIFAINEAV ESGDVGKTLS ALRSPDVGLY GVIPECGETY HSDLAEAKKK
```

D: WW domain

```
IQGAP2     VSSDGSWLKL NLHKKYDYYY NTDSKESSWV TPESCFYK
IQGAP1     GDNNSKWVKH WVKGGYYYYH NLETQEGGWD EPPNFVQN
Dystrophin TSVQGPWERA ISPNKVPYYI NHETQTTCWD HPKMTELY
C38D4.5    RDLLNGWFEY ETDVGRTFFF NKETGKSQWI PPRFIRTP
YAP-ww1    VPLPAGWEMA KTSSGQRYYL NHNDQTTTWQ DPRKAMLF
YAP-ww2    GPLPDGWEQA MTQDGEVYYI NHKNKTTSWL DPRLDPRS
```

E: IQ motifs:

```
IQGAP2-1   SEELLLRFQA TSSGPILREE FEARKSFLHE
IQGAP2-2   QEENVVKIQA FWKGYKQRKE YMHRRQTFID
IQGAP2-3   NTDSVVKIQS WFRMATARKS YLSRLQYFRD
IQGAP2-4   HNNEIVKIQS LLRANKARDD YKTLVGSENP
```

F: Coiled-coil probability:

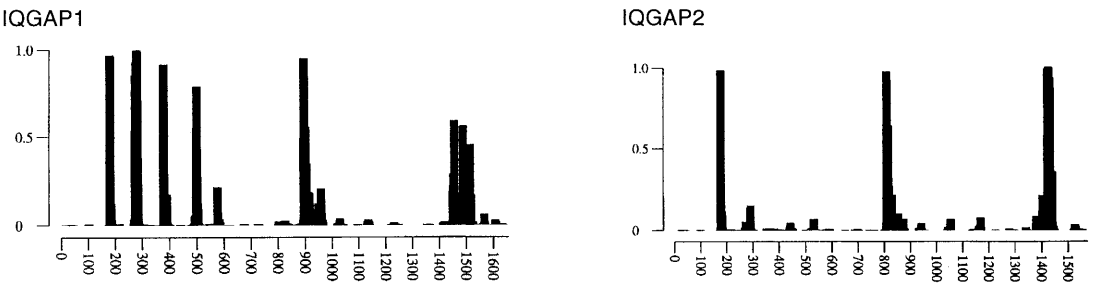

FIG. 2. Structural domains of IQGAPs. Protein sequences are presented in the one-letter amino acid code. Repeats are numbered from the N to the C terminus. (A) Schematic drawing showing the localization of domains and the percent amino acid sequence identity between IQGAPs and the indicated segments of sar1. (B) Alignment of CH domains in IQGAP2 (residues 44 to 152), IQGAP1 (GenBank accession number L33075; amino acids 47 to 155), *Drosophila* asynchronous muscle protein MP20 (Swissprot number P14318; residues 19 to 118), human proto-Vav (Swissprot number L15498; residues 4 to 115), human α-actin (GenBank accession number X15804; amino acids 33 to 131), and human filamin (GenBank accession number X53416; amino acids 45 to 145). The last two proteins each contain two CH domains, the N-terminal one of which is shown. Dots represent spaces that were introduced to optimize the alignment, which is based on a published alignment of CH domains (11). (C) IQGAP-specific IQGAP repeat motifs. The five such repeats in IQGAP2 start at amino acids 213, 302, 370, 452, and 537, respectively. The six IQGAP1 repeats start at residue 216, 304, 387, 455, 537, and 622, respectively. Database searches with the Profilesearch program (15) revealed no other occurrences of these repeats in databases current as of April 1996. (D) WW or WWP putative protein interaction domain. These approximately 38-residue motifs in IQGAP1 and -2 start at residue 679 and 594, respectively. The WW domain in human dystrophin (GenBank accession number X14298) starts at residue 3055. C38D4.4 is a Dbl-related putative Rho exchange factor from *C. elegans* (Swissprot number P46941). The single WW domain in C38D4.4 starts at amino acid 96. The two WW domains in human Yes-associated protein (YAP) (44) start at amino acids 156 and 216, respectively. (E) IQ motifs. These 30-amino-acid motifs start at IQGAP2 residue 660, 690, 720, and 750, respectively. (F) Prediction of coiled-coil regions. The plots indicate the probability that a given IQGAP1 or -2 segment will assume a coiled-coil structure and were generated with the MacStripe computer program using a 28-residue sliding window (26). This program is based on an algorithm that predicts coiled-coil regions (28). Numbers on the horizontal axis indicate amino acid residues in the two proteins.

fusion protein representing the Ras-binding CR1 segment of Raf1 (residue 1 to 259 [52]) potently inhibited p120GAP-mediated Ras-GTP hydrolysis (Fig. 5B). IQGAP2 thus showed neither GAP activity towards Ras nor evidence of interacting with H-Ras under the conditions tested. Although IQGAP2 may still interact with Ras in the presence of specific cofactors, this seems unlikely since identical results were obtained with affinity-purified IQGAP2 and with IQGAP2 present in unfractionated Sf9 cell lysates.

IQGAP2 interacts with Cdc42 and Rac1. To analyze whether IQGAP2 interacts with other Ras-related GTPases, we performed in vitro binding experiments with baculovirus IQGAP2 and a panel of GST-GTPase fusion proteins. To test for interactions, glutathione agarose-bound GTPases were loaded with a nonhydrolyzable GTP analog and incubated with IQGAP2-infected Sf9 cell lysates. After extensive washing, the presence of bound IQGAP2 was detected by immunoblotting with the anti-HA monoclonal antibody 12CA5. In these experiments,

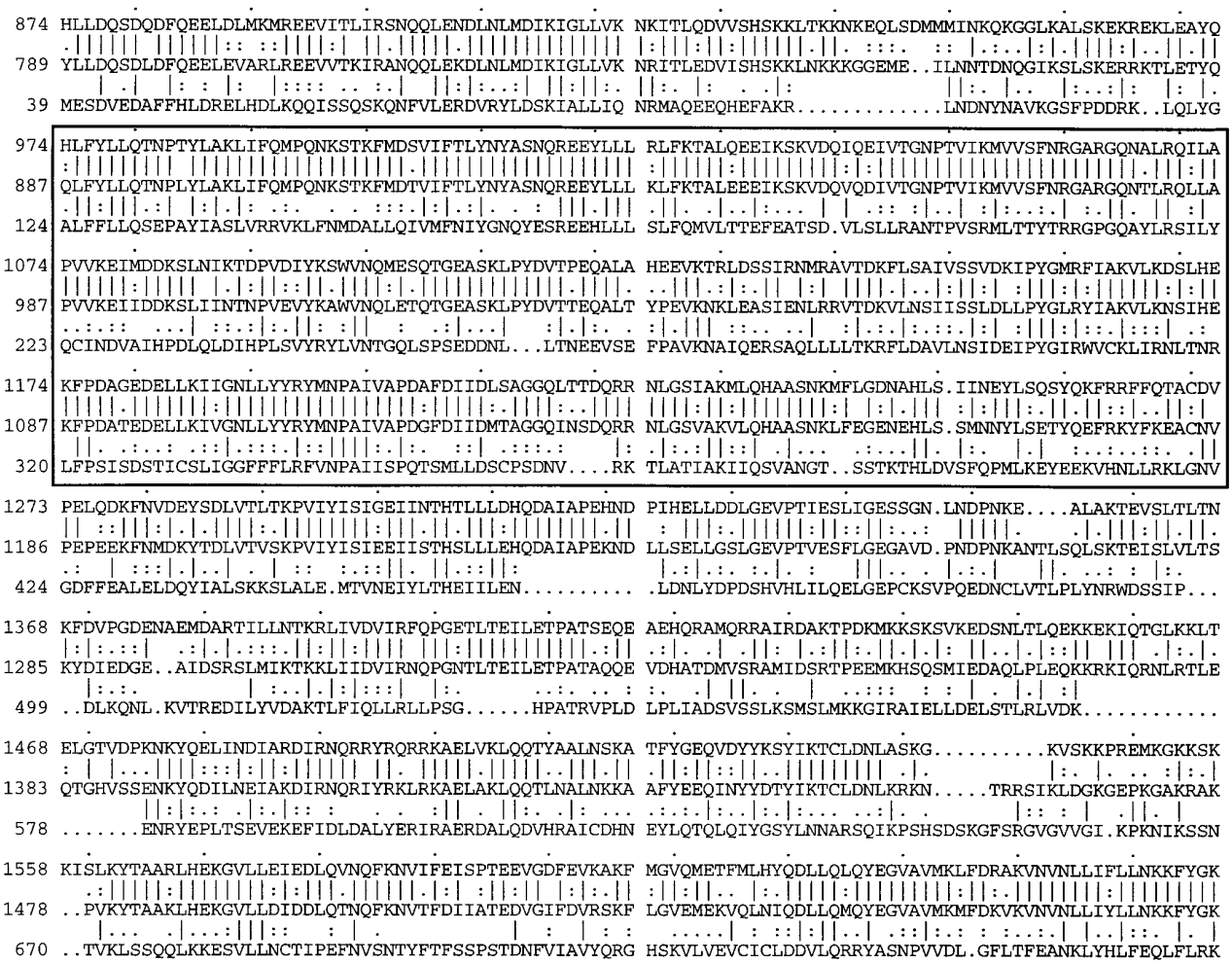

FIG. 3. Multiple sequence alignment of the homologous segments of IQGAP1, IQGAP2, and *S. pombe* sar1. The boxed region indicates the approximate extent of the protein segments that show similarity to the putative catalytic domains of RasGAPs. The alignment was generated with the GAP program (15).

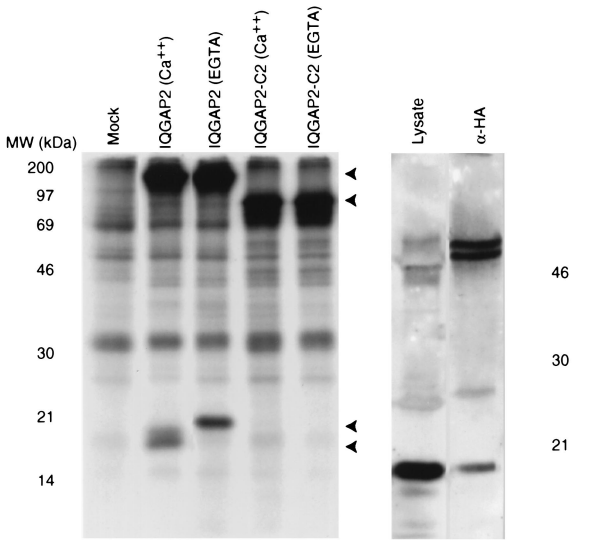

FIG. 4. IQGAP2 binds CaM. The left panel shows proteins precipitated from transfected Cos cells with the 12CA5 antibody. The upper arrows identify the 180- and 85-kDa IQGAP2 and IQGAP2-C2 proteins, respectively. The lower pair of arrows indicate the mobility shift of the IQGAP2-associated protein. The right panel shows an immunoblot containing samples of lysate of untransfected Cos cells and an anti-HA (α-HA) precipitate of IQGAP2-transfected cells. The blot was probed with an anti-bovine CaM monoclonal antibody (05-173; Upstate Biotechnology).

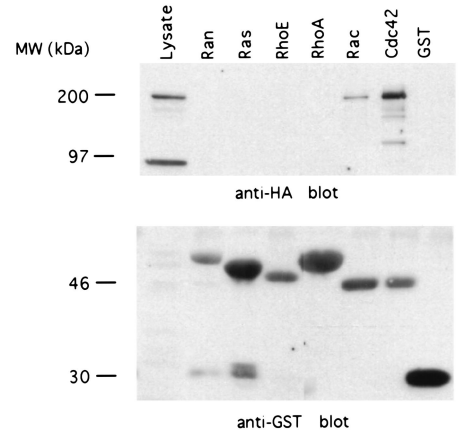

FIG. 6. IQGAP2 interacts with Cdc42 and Rac1 but not with several other members of the Ras GTPase superfamily. RhoE is a recently newly discovered member of the Rho GTPase family (19). Glutathione agarose-bound GMP-PNP-loaded GTPases were incubated with IQGAP2-infected Sf9 cell lysates, after which bound proteins were analyzed by immunoblotting with the 12CA5 anti-HA monoclonal antibody (upper panel). The lower panel shows the lower part of the same immunoblot after probing with an anti-GST antibody (GST12; Santa Cruz Biotechnology).

full-length IQGAP2 showed prominent binding to Cdc42 (G25K isotype) and to a lesser extent also to Rac1 but not to H-Ras, RhoA, RhoE, or Ran or to GST control beads (Fig. 6, upper panel). In addition, RalA, Rap1b, and TC21 also did not bind (not shown). Probing the blots with an anti-GST antibody showed that similar amounts of the fusion proteins were used in these assays (Fig. 6, lower panel).

In GAP assays similar to those described above, affinity-purified HA-IQGAP2 did not stimulate the GTPase activity of Cdc42 or Rac1, whereas a GST protein representing the catalytic segment of RhoGAP (5) reproducibly stimulated more than 80% Cdc42-GTP or Rac1-GTP hydrolysis (not shown). However, providing further proof that IQGAP2 indeed interacts with these GTPases, the intrinsic rate of Cdc42-GTP or Rac1-GTP hydrolysis showed a consistent twofold inhibition in the presence of IQGAP2 (Fig. 7A and B). This did not reflect inhibition of nucleotide dissociation by IQGAP2, as judged from similar experiments in which [α-^{32}P]GTP-loaded GTPases were used (not shown). Moreover, IQGAP2 caused a potent dosage-dependent inhibition of RhoGAP-stimulated Cdc42-GTP or Rac1-GTP hydrolysis (Fig. 7C and D). Thus, IQGAP2 may potentiate the active GTP-bound forms of these

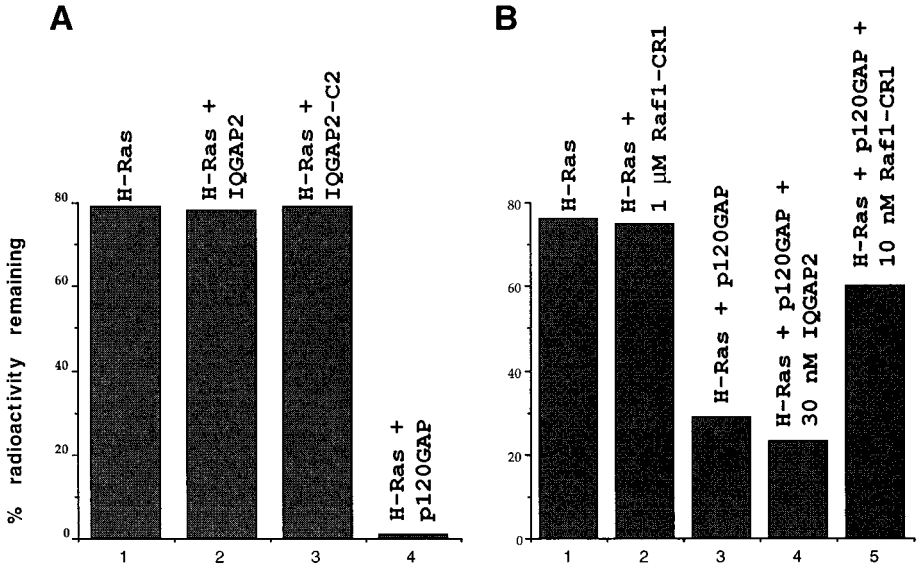

FIG. 5. IQGAP2 lacks in vitro RasGAP activity. The results of in vitro GAP assays are plotted as the percentage of H-Ras-bound radioactivity remaining after a 10-min incubation at 30°C. (A) The reactions plotted contained 6 nM thrombin-cleaved H-Ras and 60 nM GAP. (B) Inhibition of p120GAP-stimulated H-Ras GTP hydrolysis by a Raf-1 CR1 fusion protein but not by IQGAP2 is shown. The amount of p120GAP used in this assay was titrated to give 70% GTP hydrolysis after 10 min.

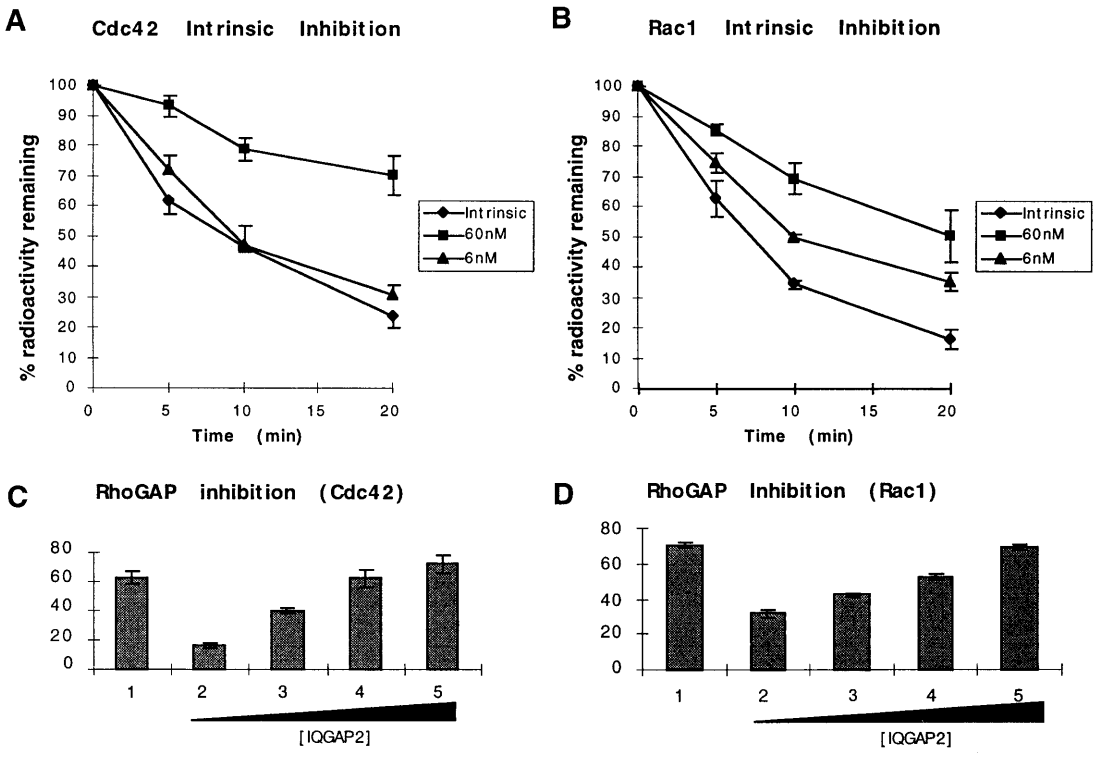

FIG. 7. IQGAP2 inhibits the intrinsic (A and B) and RhoGAP-stimulated (C and D) GTP hydrolysis rates of Cdc42 and Rac1. (C and D) The percentages of counts remaining after 5 min in the absence (bar 1) of RhoGAP or in the presence (bars 2 to 5) of 0.6 nM RhoGAP (C) or 4.5 nM RhoGAP (D) are shown. Bars 3, 4, and 5 show the effect of adding increasing concentrations (6, 18, and 60 nM, respectively) of IQGAP2.

GTPases by inhibiting their intrinsic rate of GTP hydrolysis and by interfering with their interaction with RhoGAPs.

To analyze whether IQGAP2 also interacts with Cdc42 and Rac1 when not in severe excess, we tested whether the immobilized GTPases also bound IQGAP2 in extracts of IQGAP2-expressing liver cells. Among the limited number of proteins that bind to Cdc42 and Rac1 under these conditions, a 180-kDa protein is present in IQGAP2-expressing Hep3B cells but absent from IQGAP2-deficient Focus cells (Fig. 8, lanes 1 to 4). Two polyclonal antisera directed against an N-terminal IQGAP2 peptide precipitate a protein of exactly this size from IQGAP2-expressing Hu-H7 and Hep3B cells but not from IQGAP2-deficient Focus cells, suggesting that the 180-kDa Cdc42 and Rac1 binding protein in Hep3B extracts is indeed endogenous IQGAP2 (Fig. 8, lanes 5 to 7).

To determine which part of IQGAP2 mediates the binding to Cdc42 and Rac1, we made vectors to express N-terminally and C-terminally truncated IQGAP2 proteins. The diagram in Fig. 9 shows the structure of the three truncated proteins tested, all of which included C-terminal HA tags (see Materials and Methods for a description of these constructs). Cos cells transfected with the truncated vectors produced anti-HA immunoreactive proteins of the expected sizes, although cells transfected with the two IQGAP2-C constructs consistently produced several proteins, perhaps reflecting proteolytic degradation or the use of internal translational start codons (Fig. 9). In binding assays, both full-length IQGAP2 and the IQGAP2-C1 protein showed prominent binding to Cdc42 and Rac1. The IQGAP2-N protein did not bind, indicating that IQGAP2 interacts with these GTPases via its C-terminal half. Interestingly, the IQGAP2-C2 protein, which includes almost the entire sar1-homologous segment but which differs from IQGAP2-C1 in lacking residues 711 to 826, showed marginal binding only after very long exposure times (not shown). Although improper folding of the IQGAP2-C2 protein could explain this result, it raises the interesting possibility that perhaps part of the Cdc42- and Rac1-interacting domain maps near the start or upstream of the sar1-related segment of IQGAP2. We note in this respect that IQGAP2 does not contain a consensus Cdc42 binding domain, which is present in ACK, PAK1, and the Wiskott-Aldrich syndrome protein (29, 30, 45).

To test whether IQGAP2 also interacts with Rho-family GTPases in vivo, we cotransfected Cos cells with full-length

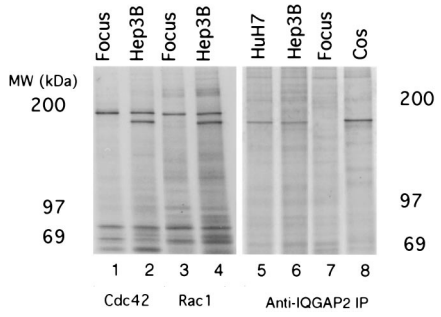

FIG. 8. Cdc42 and Rac1 interact with IQGAP2 in cell lysates. Lanes 1 to 4 show proteins bound to GMP-PNP-loaded Cdc42 and Rac1 in detergent extracts of IQGAP2-expressing Hep3B, but not in those of IQGAP2-deficient Focus cells. Lanes 5 to 8 show proteins precipitated by an antiserum made against an IQGAP2 peptide. The presence or absence of a 180-kDa immunoprecipitated protein correlated with IQGAP2 mRNA expression in all cell lines tested. The protein detected in HA-IQGAP2-transfected Cos cells (lane 8) was not detected in untransfected cells (not shown).

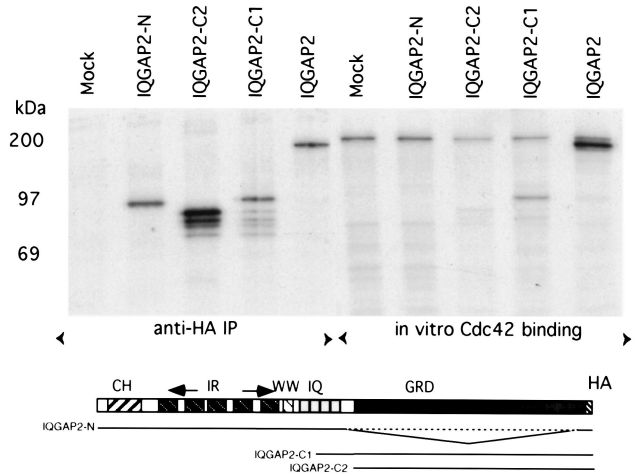

FIG. 9. Cdc42 interacts with the C-terminal half of IQGAP2. The left-hand lanes show ^{35}S-labeled proteins precipitated with the 12CA5 antibody from extracts of transiently transfected Cos cells (anti-HA IP). The right-hand lanes show labeled proteins that bind to immobilized Cdc42-GMP-PNP (in vitro Cdc42 binding). The diagram shows the structure of the proteins encoded by the three truncated expression constructs.

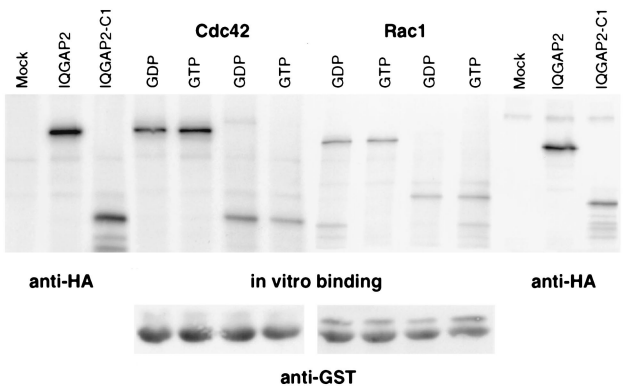

FIG. 11. IQGAP2 interacts with Cdc42 and Rac1 independent of their nucleotide binding status. The lanes labeled anti-HA show proteins precipitated from mock-transfected cells or from cells transfected with IQGAP2 or IQGAP2-C1 expression vectors. The lanes labeled in vitro binding show full-length IQGAP2 or truncated IQGAP2-C1 binding to GDP- or GMP-PNP-loaded Cdc42 or Rac1. The anti-GST immunoblots show that equivalent amounts of the GST-GTPase fusion proteins were present in these assays.

and truncated HA-IQGAP2 and Flag epitope-tagged Cdc42^{Val-12} expression vectors. Two days after transfection, lysates were prepared and potential complexes were precipitated with the 12CA5 antibody. Detergent-washed precipitates were subjected to SDS-PAGE and blotted onto nylon filters, which were probed with the M2 anti-Flag monoclonal antibody to detect the presence of tagged Cdc42. No such protein was observed in anti-HA precipitates of mock-transfected cells (not shown) or of cells transfected with the HA-IQGAP2 vector alone. However, a protein that comigrated with tagged Cdc42 coprecipitated with both full-length HA-IQGAP2 and with HA-IQGAP2-C1 (Fig. 10). We conclude that Cdc42 and IQGAP2 also form a complex in transfected cells.

Assays in which p120GAP-mediated Ras-[γ-^{32}P]GTP hydrolysis competed with either Ras-GDP or Ras-GTP demonstrate that p120GAP preferentially binds Ras in its active GTP-bound conformation (46). By contrast, in similar assays

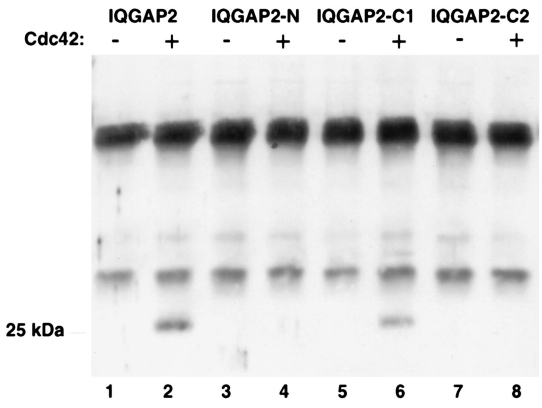

FIG. 10. Cdc42 coprecipitates with IQGAP2 from transfected cells. Cos cells were transfected with the four expression constructs indicated, either in the presence (+) or absence (−) of a Flag-tagged Cdc42 expression vector. Flag-tagged Cdc42, detected with the M2 antibody (Kodak), coprecipitates with IQGAP2 and IQGAP2-C1 but not with IQGAP2-N. Coprecipitation of Cdc42 with the shorter IQGAP2-C2 protein is observed only after very long exposure times.

RhoGAP showed only a twofold preference for Cdc42-GTP over Cdc42-GDP (27). To test whether the binding of IQGAP2 to Cdc42 or Rac1 depends on the nucleotide binding status of the GTPases, we repeated the in vitro binding experiment after loading the immobilized GTPases with either GDP or nonhydrolyzable GTP analogs. Under these experimental conditions, full-length IQGAP2 showed no consistent differential binding to Cdc42 or Rac1 in their GDP- or GMP-PNP- or γ-S-GTP-bound forms, and identical results were obtained with the IQ GAP2-C1 protein (Fig. 11).

DISCUSSION

We previously identified human IQGAP1 as a protein related to a RasGAP homolog from *S. pombe* (48). Here we report the identification and characterization of a 62% identical human protein with a very similar overall structure. Among the most striking features shared between IQGAP1 and -2 is a C-terminal 700-amino-acid region displaying similarity to *S. pombe* sar1. However, in spite of finding approximately 50% amino acid sequence similarity to almost the entire sar1 protein, we have found no evidence that IQGAP2 stimulates the activity of or even interacts with H-Ras and several close relatives in vitro. Instead, the C-terminal half of IQGAP2 binds Cdc42 and Rac1 without stimulating the activity of these Rho-related GTPases.

We previously reported that a truncated GST-IQGAP1 fusion protein did not stimulate the GTPase activity of Ras but did cause a twofold increase in filter retention of H-Ras but not of RhoA (48). Because the increased filter binding might have been caused by aberrant folding or by poor solubility of the fusion protein, we used full-length baculovirus IQGAP2 proteins in the present study, in which we observed no similar effect. Indeed, others recently identified IQGAP1 as a Cdc42 binding protein without obvious affinity for Ras (22a), which suggests that our previous result might not have reflected a property of full-length IQGAP1.

Several points about the interaction between IQGAP2 and Cdc42/Rac1 are worth noting. First, although IQGAP2 does not appear to be a GAP for Cdc42 and Rac1, the protein in in vitro assays causes a reproducible dosage-dependent inhibition of both the intrinsic and the RhoGAP-stimulated Cdc42 and Rac1 GTP hydrolysis. IQGAP2, therefore, can modulate the

activity of Cdc42 and Rac1 by inhibiting their intrinsic rate of GTP hydrolysis and by preventing their interaction with Rho GAPs. Secondly, both full-length and truncated IQGAP2 binds Cdc42 and Rac1 apparently independent of their nucleotide binding status. Although our assays do not rule out the possibility that IQGAP2 binds GDP- or GTP-loaded GTPases with different affinities under nonsaturating conditions, our results suggest that IQGAP2 recognizes GTPase segments that do not undergo a major conformational change upon GTP hydrolysis. We note in this respect that while GTP-dependent binding is often used to argue for a potential effector role, a constitutively bound protein may still serve as an effector, after being activated by the conformational change that accompanies GTPase-GTP hydrolysis. However, since the N-terminal halves of IQGAPs harbor several domains that have been implicated as binding sites for other proteins, it is perhaps more likely that IQGAPs play roles in recruiting components of Cdc42- and Rac1-controlled signaling pathways and in properly localizing these components within the cell.

Upstream of their sar1-homologous segments, IQGAPs are highly modular in structure (Fig. 2A). Indeed, this part of IQ GAP1 and -2 is almost entirely occupied by four types of domains, three of which have been recognized as protein binding motifs in other instances. Most intriguingly, IQGAP1 and -2 each harbor a so-called CH domain near the N terminus (Fig. 2B). We previously noted that this segment of IQGAP1 is most closely related to a *Drosophila* muscle protein called MP20 (48), which is a member of the calponin family of actin and CaM binding proteins (4, 50). A more detailed analysis has since revealed that this part of IQGAP1 and -2 resembles F-actin binding domains present near the N-termini of several proteins, including members of the fimbrin, filamin, and spectrin families (11). This is an interesting finding, since Cdc42, Rac, and Rho have been implicated in pathways leading to the generation of specific polymerized actin structures (37, 40, 41).

Database searches with the CH segment of IQGAP2 reveal that the Vav proto-oncoprotein harbors a similar sequence at its N terminus (Fig. 2B). This is intriguing, because Vav includes a Dbl-related Rho GTPase exchange factor domain (16) and because a deletion within the CH domain is responsible for the oncogenic activation of Vav (25), suggesting a functionally important role for this segment.

Downstream of their CH domain, IQGAP1 and -2 harbor six and five copies, respectively, of a novel 50- to 55-amino-acid repeat which has not yet been recognized in other proteins (Fig. 2C). Immediately downstream of this repeat array, each IQGAP harbors a single so-called WW or WWP motif (3, 44). Similar motifs are also present in dystrophin and a variety of other proteins, including a *Caenorhabditis elegans* Dbl-related protein called 38D4 (49). WW domains mediate binding to proline-rich peptides, suggesting that they might functionally resemble SH3 domains (12, 44).

IQGAP1 and -2 each also harbor four closely spaced IQ motifs, which are 30-amino-acid domains characterized by consecutive isoleucine and glutamine residues. Initially identified as motifs that mediate calcium-independent CaM binding in neuromodulin/GAP43/BF-50 (1), IQ motifs have since been identified as binding sites for CaM and related EF-hand proteins in a variety of proteins, including conventional and unconventional myosins (13, 14). Since our results indicate that IQGAP1 and -2 both bind CaM, these proteins could provide a link between signaling pathways mediated by Ca^{2+}-CaM and Rho-related GTPases. Since the signaling pathways controlled by Ras and Rho family members are believed to be tightly linked, it also seems notable that calcium regulation of the activity of the brain-specific Ras exchange factor RasGRF involves CaM bound via an IQ motif (17).

The single Ras homolog of *S. pombe* is not essential, but *ras1*-deficient cells have a round rather than an elongated shape, fail to initiate conjugation, and are defective in sporulation. Mutants harboring an activated $ras1^{Val\text{-}17}$ allele fail to conjugate but are otherwise normal (20, 35). The only known RasGAP-related protein from *S. pombe* was identified as the product of a gene whose disruption caused a phenotype similar to that of the activated *ras1* mutant (23) or as a protein whose overexpression suppressed the $ras1^{Val\text{-}17}$ conjugation defects (47). The latter is an unusual finding, since mammalian Ras GAPs do not (51), or only very inefficiently (36), suppress cell transformation by Ras mutants. However, although no direct proof that sar1 stimulates the GTPase activity of ras1 has been reported, and although sar1-related IQGAPs show no GAP activity towards Ras, several observations are most easily explained by assuming that sar1 indeed has RasGAP activity. For example, the expression of mammalian p120GAP suppressed the conjugation defect of a *sar1*-deficient mutant. Furthermore, sar1 rescues the heat shock-sensitive phenotype of a budding yeast *ira*-deficient mutant (47). However, since Ras-mediated signaling and Rho-mediated signaling in *S. pombe* (31) and in mammals (39) are intimately linked, the formal possibility that sar1 exerts some of its effects by interacting with Rho-family GTPases exists. For this reason it should be interesting to determine whether sar1 stimulates the GTPase activity of *S. pombe* ras1 or whether this protein interacts with the *S. pombe* Cdc42 homolog.

ACKNOWLEDGMENTS

This work was supported by Public Health Service grants NS31747 and AR16265E21. C.W.L. was the recipient of a Fuller Fellowship from the Massachusetts Chapter of the American Cancer Society.

We are grateful to Rick Cerione, Channing Der, Alan Hall, Ian Macara, Jeffrey Settleman, Qing-Ping Weng, and Xian-feng Zhang for GTPase, GAP, and Raf-1 fusion proteins, to Sue Slaugenhaupt and Jack Wands for somatic cell hybrid DNAs and liver cell lines, and to Inge The and Jeffrey Settleman for helpful discussions.

REFERENCES

1. **Alexander, K. A., B. T. Wakim, G. S. Doyle, K. A. Walsh, and D. R. Storm.** 1988. Identification and characterization of the calmodulin-binding domain of neuromodulin, a neurospecific calmodulin-binding protein. J. Biol. Chem. **263:**7544–7549.
2. **Altschul, S. F., W. Gish, W. Miller, E. W. Myers, and D. J. Lipman.** 1990. Basic local alignment search tool. J. Mol. Biol. **215:**403–410.
3. **André, B., and J.-Y. Springdael.** 1994. WWP, a new amino acid motif present in single and multiple copies in various proteins including dystrophin and the SH3-binding Yes-associated protein YAP65. Biochem. Biophys. Res. Commun. **205:**1202–1205.
4. **Ayme-Southgate, A., P. Lasko, C. French, and M. L. Pardue.** 1989. Characterization of the gene for mp20: a Drosophila muscle protein that is not found in asynchronous oscillatory flight muscle. J. Cell Biol. **108:**521–531.
5. **Barfod, E. T., Y. Zheng, W. J. Kuang, M. J. Hart, T. Evans, R. A. Cerione, and A. Ashkenazi.** 1993. Cloning and expression of a human CDC42 GTPase-activating protein reveals a functional SH3-binding domain. J. Biol. Chem. **268:**26059–26062.
6. **Boguski, M. S., and F. McCormick.** 1993. Proteins regulating Ras and its relatives. Nature (London) **366:**643–654.
7. **Bollag, G., and F. McCormick.** 1991. Differential regulation of rasGAP and neurofibromatosis gene product activities. Nature (London) **351:**576–579.
8. **Bourne, H. R., D. A. Sanders, and F. McCormick.** 1990. The GTPase superfamily: a conserved switch for diverse cellular functions. Nature (London) **348:**125–132.
9. **Bourne, H. R., D. A. Sanders, and F. McCormick.** 1991. The GTPase superfamily: conserved structure and molecular mechanism. Nature (London) **349:**117–127.
10. **Burgess, W. H., D. K. Jemiolo, and R. H. Kretsinger.** 1980. Interaction of calcium and calmodulin in the presence of sodium dodecyl sulfate. Biochim. Biophys. Acta **623:**257–270.

11. **Castresana, J., and M. Saraste.** 1995. Does Vav bind to F-actin through a CH domain? FEBS Lett. **374:**149–151.
12. **Chan, D. C., M. T. Bedford, and P. Leder.** 1996. Formin binding proteins bear WWP/WW domains that bind proline-rich peptides and functionally resemble SH3 domains. EMBO J. **15:**1045–1054.
13. **Cheney, R. E., and M. S. Mooseker.** 1992. Unconventional myosins. Curr. Opin. Cell Biol. **4:**27–35.
14. **Cheney, R. E., M. K. O'Shea, J. E. Heuser, M. V. Coelho, J. S. Wolenski, E. M. Espreafico, P. Forscher, R. E. Larson, and M. S. Mooseker.** 1993. Brain myosin-V is a two-headed unconventional myosin with motor activity. Cell **75:**13–23.
15. **Devereux, J., P. Haeberli, and O. Smithies.** 1984. A comprehensive set of sequence analysis programs for the VAX. Nucleic Acids Res. **12:**387–395.
16. **Eva, A., and S. A. Aaronson.** 1985. Isolation of a new human oncogene from a diffuse B-cell lymphoma. Nature (London) **316:**273–275.
17. **Farnsworth, C. L., N. W. Freshney, L. B. Rosen, A. Ghosh, M. E. Greenberg, and L. A. Feig.** 1995. Calcium activation of Ras mediated by neuronal exchange factor Ras-GRF. Nature (London) **376:**524–527.
18. **Feinberg, A. P., and B. Vogelstein.** 1983. A technique for radiolabeling DNA restriction fragments to high specific activity. Anal. Biochem. **132:**6–13.
19. **Foster, R., K.-Q. Hu, Y. Lu, K. M. Nolan, J. Thissen, and J. Settleman.** 1996. Identification of a novel human Rho protein with unusual properties: GTPase deficiency and in vivo farnesylation. Mol. Cell. Biol. **16:**2689–2699.
20. **Fukui, Y., T. Kozasa, Y. Kaziro, T. Takeda, and M. Yamamoto.** 1986. Role of a ras homolog in the life cycle of *Schizosaccharomyces pombe*. Cell **44:** 329–336.
21. **Geissler, E. N., M. Liao, J. D. Brook, F. H. Martin, K. M. Zsebo, D. E. Housman, and S. J. Galli.** 1991. Stem cell factor (SCF), a novel hematopoietic growth factor and ligand for c-kit tyrosine kinase receptor, maps on human chromosome 12 between 12q14.3 and 12qter. Somatic Cell Mol. Genet. **17:**207–214.
22. **Hall, A., and A. J. Self.** 1986. The effect of Mg^{2+} on the guanine nucleotide exchange rate of $p21^{N\text{-}ras}$. J. Biol. Chem. **261:**10963–10965.

22a. **Hart, M. J., M. G. Callow, B. Souza, and P. Polakis.** 1996. IQGAP1, a calmodulin-binding protein with a rasGAP-related domain, is a potential effector for cdc42Hs. EMBO J. **15:**2997–3005.

23. **Imai, Y., S. Miyake, D. A. Hughes, and M. Yamamoto.** 1991. Identification of a GTPase-activating protein homolog in *Schizosaccharomyces pombe*. Mol. Cell. Biol. **11:**3088–3094.
24. **Janknecht, R., G. de Martynoff, J. Lou, R. A. Hipskind, A. Nordheim, and H. G. Stunnenberg.** 1991. Rapid and efficient purification of native histidine-tagged protein expressed by recombinant vaccinia virus. Proc. Natl. Acad. Sci. USA **88:**8972–8976.
25. **Katzav, S., J. L. Cleveland, H. E. Heslop, and D. Pulido.** 1991. Loss of the amino-terminal helix-loop-helix domain of the *vav* proto-oncogene activates its transforming potential. Mol. Cell. Biol. **11:**1912–1920.
26. **Knight, A. E.** 1994. The diversity of myosin-like proteins. Ph.D. thesis. Cambridge University, Cambridge.
27. **Lancaster, C. A., P. M. Taylor-Harris, A. J. Self, S. Brill, H. E. van Erp, and A. Hall.** 1994. Characterization of rhoGAP. A GTPase-activating protein for rho-related small GTPases. J. Biol. Chem. **269:**1137–1142.
28. **Lupas, A., M. van Dyke, and J. Stock.** 1991. Predicting coiled-coils from protein sequences. Science **252:**1162–1164.
29. **Manser, E., T. Leung, H. Salihuddin, L. Tan, and L. Lim.** 1993. A non-receptor tyrosine kinase that inhibits the GTPase activity of p21cdc42. Nature (London) **363:**364–367.
30. **Manser, E., T. Leung, H. Salihuddin, Z.-S. Zhao, and L. Lim.** 1994. A brain serine/threonine protein kinase activated by Cdc42 and Rac1. Nature (London) **367:**40–46.
31. **Marcus, S., A. Polverino, E. Chang, D. Robbins, M. H. Cobb, and M. H. Wigler.** 1995. Shk1, a homolog of the *Saccharomyces cerevisiae* Ste20 and mammalian $p65^{PAK}$ protein kinases, is a component of a Ras/Cdc42 signaling module in the fission yeast *Schizosaccharomyces pombe*. Proc. Natl. Acad. Sci. USA **92:**6180–6184.
32. **McCormick, F.** 1989. *ras* GTPase activating protein: signal transmitter and signal terminator. Cell **56:**5–8.
33. **Morgenstern, J. P., and H. Land.** 1990. A series of mammalian expression vectors and characterization of their expression of a reporter gene in stably and transiently transfected cells. Nucleic Acids Res. **18:**1068.
34. **Murthy, A. E., A. Bernards, D. Church, J. Wasmuth, and F. F. Gusella.** Identification and characterization of two novel TPR containing genes. DNA Mol. Biol., in press.
35. **Nadin-Davis, S., A. Nasin, and D. Beach.** 1986. Involvement of ras in sexual differentiation but not in growth control in fission yeast. EMBO J. **5:**2963–2971.
36. **Nakafuku, M., M. Nagamine, A. Ohtoshi, K. Tanaka, A. Toh-E, and Y. Kaziro.** 1993. Suppression of oncogenic Ras by mutant neurofibromatosis type 1 genes with single amino acid substitutions. Proc. Natl. Acad. Sci. USA **90:**6706–6710.
37. **Nobes, C. D., and A. Hall.** 1995. Rho, Rac, and Cdc42 GTPases regulate the assembly of multimolecular focal complexes associated with actin stress fibers, lamellipodia, and filipodia. Cell **81:**53–62.
38. **Pelletier, J., J. D. Brook, and D. E. Housman.** 1991. Assignment of two of the translation initiation factor-4E (EIF4EL1 and EIF4EL2) genes to human chromosomes 4 and 20. Genomics **10:**1079–1082.
39. **Qiu, R.-G., J. Chen, D. Kirn, F. McCormick, and M. Symons.** 1995. An essential role for Rac in Ras transformation. Nature (London) **374:**457–459.
40. **Ridley, A. J., and A. Hall.** 1992. The small GTP-binding protein *rho* regulates assembly of focal adhesions and actin stress fibers in response to growth factors. Cell **70:**389–399.
41. **Ridley, A. J., H. F. Paterson, C. L. Johnston, D. Diekmann, and A. Hall.** 1992. The small GTP-binding protein *rac* regulates growth factor-induced membrane ruffling. Cell **70:**401–410.
42. **Sambrook, J., E. F. Fritsch, and T. Maniatis.** 1989. Molecular cloning: a laboratory manual, 2nd ed. Cold Spring Harbor Laboratory Press, Cold Spring Harbor, N.Y.
43. **Snijders, A. J., V. H. Haase, and A. Bernards.** 1993. Four tissue-specific mouse *ltk* mRNAs predict tyrosine kinases that differ upstream of their transmembrane segment. Oncogene **8:**27–35.
44. **Sudol, M., H. I. Chen, C. Bougeret, A. Einbond, and P. Bork.** 1995. Characterization of a novel protein-binding module—the WW domain. FEBS Lett. **369:**67–71.
45. **Symons, M., J. M. J. Derry, B. Karlak, S. Jiang, V. Lemahieu, F. McCormick, U. Francke, and A. Abo.** 1996. Wiskott-Aldrich syndrome protein, a novel effector for the GTPase CDC42Hs, is implicated in actin polymerization. Cell **84:**723–734.
46. **Vogel, U. S., R. A. F. Dixon, M. D. Schaber, R. E. Diehl, M. S. Marshall, E. M. Scolnick, I. S. Sigal, and J. B. Gibbs.** 1988. Cloning of bovine GAP and its interaction with oncogenic *ras* p21. Nature (London) **335:**90–93.
47. **Wang, Y., M. Boguski, M. Riggs, L. Rodgers, and M. Wigler.** 1991. *Sar1*, a gene from *Schizosaccharomyces pombe* encoding a protein that regulates ras1. Cell Regul. **2:**453–465.
48. **Weissbach, L., J. Settleman, M. F. Kalady, A. J. Snijders, A. E. Murthy, Y.-X. Yan, and A. Bernards.** 1994. Identification of a human rasGAP-related protein containing calmodulin-binding motifs. J. Biol. Chem. **269:**20517–20521.
49. **Wilson, R., R. Ainscough, K. Anderson, C. Baynes, M. Berks, J. Bonfield, J. Burton, M. Connell, T. Copsey, J. Cooper, et al.** 1994. 2.2 Mb of contiguous nucleotide sequence from chromosome III of C. elegans. Nature (London) **368:**32–38.
50. **Winder, S. J., and M. P. Walsh.** 1993. Calponin: thin filament-linked regulation of smooth muscle contraction. Cell. Signalling **5:**677–686.
51. **Zhang, K., J. E. DeClue, W. C. Vass, A. G. Papageorge, F. McCormick, and D. R. Lowy.** 1990. Suppression of c-*ras* transformation by GTPase-activating protein. Nature (London) **346:**754–756.
52. **Zhang, X.-F., J. Settleman, J. M. Kyriakis, E. Takeuchi-Suzuki, S. J. Elledge, S. Marshall, J. T. Bruder, U. R. Rapp, and J. Avruch.** 1993. Normal and oncogenic $p21^{ras}$ proteins bind to the amino-terminal regulatory domain of c-Raf-1. Nature (London) **364:**308–313.